

October 31, 2001

Water Quality Co-Benefits of Greenhouse Gas Reduction Incentives in Agriculture and Forestry

Draft Report

Prepared for

Benjamin DeAngelo, OAR/OAP/PPD
U.S. Environmental Protection Agency
499 S. Capitol Street, SW
Washington, DC 20024

Prepared by

Timothy Bondelid
Brian Murray
Subhrendu Pattanayak
Dana Lawrence
Jui-Chen Yang
RTI

EPA Contract Number 68-C-01-001
RTI Project Number 92U-08000.000.011

Water Quality Co-Benefits of Greenhouse Gas Reduction Incentives in Agriculture and Forestry

Draft Report

Prepared for

Benjamin DeAngelo, OAR/OAP/CPPD
U.S. Environmental Protection Agency
499 S. Capitol Street, SW
Washington, DC 20024

Prepared by

Timothy Bondelid
Brian Murray
Subhrendu Pattanayak
Dana Lawrence
Jui-Chen Yang
RTI
Research Triangle Park, NC 27709

Bruce McCarl
Dhazn Gillig
Texas A&M University and McCarl and Associates

EPA Contract Number 68-C-01-001
RTI Project Number 92U-08000.000.011

October 31, 2001

ASSESSING WATER QUALITY CO-BENEFITS OF GREENHOUSE GAS REDUCTION STRATEGIES IN AGRICULTURE AND FORESTRY

1. Introduction

There is growing interest in the role that agricultural practices and forest establishment can play in preventing global warming. The agriculture and forestry sectors can contribute to greenhouse gas (GHG) mitigation through (1) carbon sequestration, (2) reduction of GHG emissions from management practices, and (3) substitution of renewable biomass based products for materials and processes that generate GHG emissions through fossil fuel combustion.

Terrestrial or biological carbon sequestration removes carbon dioxide (CO₂) from the atmosphere and stores it as carbon in biomass and soils. Typical land-use practices that preserve and enhance terrestrial carbon storage include switching from conventional to low- or no-till agriculture, converting agricultural and pasture land to forests, protecting forests, lengthening rotation periods of the timber-harvest cycle, and establishing riparian buffers with forests or other native vegetation. Other forms of GHG mitigation from agriculture include reductions in N₂O from fertilizer use and reductions in methane (CH₄) from livestock management.

The practice that sequester carbon have substantial overlap with practices that have historically been used to improve environmental quality by reducing farm-generated nonpoint source pollution. As such, widespread adoption of a carbon program employing these options should simultaneously yield ancillary environmental benefits. Little quantitative work has been done to assess the ancillary effects of these land use practices on water quality and quantity, soil quality, soil erosion, biodiversity, and acidification. Nevertheless, the Intergovernmental Panel on Climate Change (IPCC) Special Report on Land Use, Land-Use Change and Forestry suggests most land-use change and forestry (LUCF) practices for GHG mitigation would likely lead to broader environmental benefits, though there may be tradeoffs between GHG benefits and environmental quality in some cases.

This project represents an initial attempt to better understand the synergies and possible tradeoffs between terrestrial GHG mitigation strategies and the nation's water quality objectives. Such information may help EPA and other parties better identify land-use practices that have the greatest potential for both climate protection and water quality improvement. This analysis involves a first-of-its-kind linkage between the modeling tools employed by EPA Office of Water (OW) for water quality analyses and Office of Air and Radiation (OAR) for analysis of

sequestration strategies in forestry and agriculture. The project leverages significant efforts that EPA has invested in the development and use of models in different parts of the Agency to address distinct, but related, environmental problems. We proceed with an evaluation of policies targeted at GHG reductions and evaluate the ancillary water quality effects. However, the problem, in essence, could be viewed in reverse. That is, policies aimed primarily at water quality improvements may provide ancillary GHG mitigation benefits. Regardless, they are joint effects.

The model used by OAR's Methane and Sequestration Branch to simulate mitigation policies in the agriculture and forestry sectors includes the Agricultural Sector Model-Greenhouse Gases (ASMGHG), developed by Dr. Bruce McCarl and his research staff. ASMGHG is a national-level model of the U.S. agricultural sector, with linkages to the forest sector through land markets.¹ ASMGHG also considers international trade in agricultural products. It includes considerable detail on agricultural production, particularly with regard to practices that impact carbon sequestration, CO₂ emissions, and non-CO₂ greenhouse gases reporting strategy use in 63 U.S. regions.

The National Water Pollution Control Assessment Model (NWPCAM) is a national-scale modeling system developed by RTI that is used to simulate water quality at a macro scale and is specifically designed to evaluate various policies, such as effects of Clean Water Act and proposed rules on Animal Feeding Operations. It can generate water quality estimates at either a Reach File Version 1 (RF1) level of detail (~630,000 miles of rivers and streams), or at an RF3 level (>3 million miles of rivers and streams) of detail. This work assignment thus leverages prior efforts by EPA, especially work for the Office of Science and Technology, the Office of Wastewater Management (NWPCAM), and OAR (ASM). The work also uses a linkage model developed by McCarl in conjunction with the USDA NRCS which allocates ASMGHG projections of cropping activities by 63 U.S. regions down to the level of U.S. counties allowing computation of emission coefficients that may be used in NWPCAM.

The report continues with a brief summary of the technical approach used to link the two modeling systems to jointly produce estimates of GHG reduction and ancillary water quality effects. That is followed by a discussion of results from the ASMGHG model runs, a description of the NWPCAM results, and a summary of results and suggestions for future research.

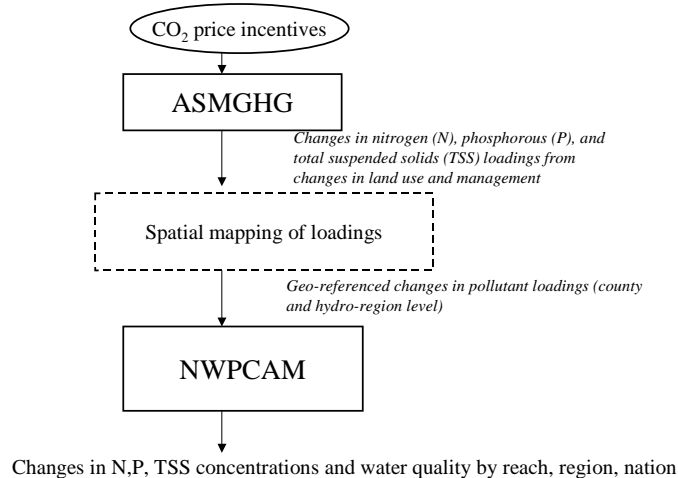
2. Technical Approach for Evaluating GHG Policy Scenarios

¹ A related model, FASOM, also co-developed by Dr. McCarl, more explicitly links the agricultural and forest sectors. ASMGHG was used for this analysis because of its wider coverage of GHGs and higher level of spatial detail.

To simulate the link between GHG mitigation actions in agriculture and forestry to changes in water quality, we integrated results from ASMGHG with NWPCAM databases to estimate changes in delivery of nitrogen (N), phosphorous (P), and total suspended solids (TSS) into the nation’s waters along with indicators of the change in water quality these deliveries may make. We compared “baseline” conditions (circa late 1990's) with two scenarios (circa 2020), which reflect two different prices for sequestered carbon (\$2.72 and \$15 per ton of CO₂ equivalent), as reflected in ASMGHG outputs (e.g., land use and agricultural practices).

An overview of the model system overview is presented in Figure 1. Among other things, ASMGHG allocates land between agricultural and forest uses based on relative economic returns, inclusive of returns to sequestered carbon. Thus, it provided change data on land-use, cropping and livestock holdings for the two scenarios each of the 63 regions within the model. While this is a fairly fine level of spatial detail for economic analysis, it is not sufficiently detailed for water quality modeling. Thus, additional spatial mapping was required. For N, P, and TSS loadings from cropland, ASMGHG results were further broken down to the county level using an auxiliary multiple objective programming model which allocates the ASMGHG 63 region level crop mix changes to counties in a fashion most consistent with the USDA’s Natural Resource Inventory (NRI) and Agricultural Census observations on observed county level cropping patterns.

Figure 1. Model Process Overview



NWPCAM contains USGS land use/cover data at a one (1) square kilometer grid cell basis nationwide that are linked both to counties and to the RF3 river network to model water quality. Because ASMGHG and NWPCAM use different land use categorizations, we built a

cross-link to ensure that land use categories used in ASMGHG are reasonably mapped to the land use/cover categories used in NWPCAM.² The percentage change in loadings of the selected pollutants (from ASMGHG) are processed in NWPCAM using extremely data-intensive procedures because NWPCAM takes every 1 square kilometer grid cell loading, transports it to the nearest RF3 Reach, and then transports and decays the combined loadings (including, for instance point sources) down the river network.

We use percentage changes instead of absolute changes because ASMGHG and NWPCAM use very different methods for estimating loadings. It would be extremely difficult to resolve these differences on an absolute basis and then arrive at the “truth”. Estimating nonpoint source (NPS) loadings is complex and the export coefficient methodology used in NWPCAM is a highly scale-dependent modeling approach. For instance, export from a 1 hectare field is very different from export from a 100 hectare watershed. The export coefficients represent not only field-scale processes but also transport and decay processes *at the scale being modeled*. Resolving scale differences between ASM and NWPCAM is beyond the scope of this first round of analyses; it would be most interesting at some later date to perform further analyses to see if the NWPCAM loadings can be enhanced by the ASM estimates.

3. ASMGHG Results

The ASMGHG sector model used is a mathematical programming based, price endogenous representation of the agricultural sector (ASM - McCarl et al., 2000b, Chang et al., 1992), modified to include GHG emissions accounting by Schneider, 2000, and hereafter called ASMGHG). ASMGHG was also expanded to include forestry possibilities for carbon production by including data on land diversion, carbon production and economic value of forest products as generated from a forestry sector model (FASOM-Adams et al., 1996, Alig et al., 1998) using 30-year average results over the 2000-2029 period. ASMGHG depicts production, consumption and international trade in 63 U.S. regions of 22 traditional and 3 biofuel crops, 29 animal products, and more than 60 processed agricultural products. Modeled environmental impacts include levels of greenhouse gas emission or absorption for carbon dioxide, methane, and nitrous oxide; surface, subsurface, and ground water pollution for nitrogen and phosphorous; and soil erosion. ASMGHG simulates the market and trade equilibrium in agricultural markets of the U.S. and 28 major foreign trading partners. Domestic and foreign supply and demand conditions are considered, as are regional production conditions and resource endowments. The market equilibrium reveals commodity and factor prices, levels of domestic production, export

² We were unable to map 5 of the approximately 3000 counties because of imperfect overlap of the two model data bases, reflecting somewhat incomplete coverage. However, this represents a very small approximation error (less than 0.2%) in coverage.

and import quantities, GHG emissions management strategy adoption, resource usage, and environmental impact indicators.

3.1 National-level Results

We compared ASMGHG output from “baseline” conditions circa late 1990's (no GHG price) and two scenarios circa 2020 that reflected two different prices for sequestered or released GHGs (\$2.72 and \$15 per ton of CO₂ equivalent). The introduction of these incentives causes ASMGHG to change its equilibrium allocation of land use, management practices within uses, commodity production and consumption, trade flows and environmental loadings. The scenario results are presented at the national level in Table 1.³

3.1.1 Economic results

Key among the national economic results generated by the GHG incentive payments are

- Decline in agricultural production (traditional crop production offset partially by bio-fuel production and limited afforestation)
- Rise in agricultural prices
- Consumer welfare losses due to higher prices
- Producer welfare gains due to higher food prices and market or government payments for the new commodity GHG offsets
- Exports and export earnings suffer with the U.S. facing a worsening balance of payments.

Producers gain by about \$100 million and \$6.0 billion, respectively, under the low and high price scenarios. Taking into account consumer losses, the total welfare costs of the incentive system would be about \$1 - 1.5 billion which would need to be balanced by gains in other parts of the economy in terms of reduced GHG damages, reduced mitigation costs in the non-agricultural sectors, and the economic value of the co-benefits.

³ Please note that the ASMGHG runs used in this exercise were generated in June, 2001. Since then, ASMGHG has undergone some modification and current results may differ. To see more recent results from ASMGHG, please refer to a synthesis of national-level model results for GHG mitigation in forestry and agriculture presented at the First Forestry and Agriculture Greenhouse Gas Modeling Forum (<http://foragforum.rti.org/papers/index.cfm>).

3.1.2 GHG mitigation results

Table 1 also shows that total GHG emissions from agriculture decline from about 128.5 MM tons of *carbon* equivalent (MMTCE) per year in the baseline to 71.2 MMTCE at the low price (a GHG reduction benefit of 57.3 MMTCE/yr). At the high CO₂ price, agriculture becomes a net sink of -48.8 MMTCE/year (GHG mitigation of 177.3 MMTCE/year). All species of GHG are mitigated by the incentive responses, but the effects are most dramatic for CO₂ with low- or no-tillage crop management occurring at the low price and biofuel offsets kicking in at the higher price.

3.1.3 Land use and other environmental effects

Associated with these LULC changes are loadings of phosphorous (P), nitrogen (N), erosion or total suspended solids (TSS), potassium (K), pesticide (Ps) and manure (M). The following changes in key environmental variables are found to occur at the national level across all forms of agriculture (crop and livestock),

- Land Use
 - Cropland declines
 - Pasture land and forest land increases

- Irrigated acres and water use declines

- Water pollutant loadings are altered
 - Erosion is reduced, retaining more of the soil stock
 - N and P decline at both prices
 - Potassium (K) rises slightly at the low price and declines at the high price

- Pesticide use declines.

In addition, there are factors outside these model results that may have important environmental consequences. Increased carbon stocks, land conversion to grasslands and reliance on biofuels inherent in some of the solutions may alter the long run soil productivity as increased soil carbon may enhance productivity, retain nutrients reducing need for fertilizer, and hold more water reducing drought sensitivity and water requirements. Moreover, changes in land use and land management can alter the biodiversity of the landscape's flora and fauna. These are potentially important factors to consider in future analyses.

3.2 Regional results: GHG mitigation and pollutant loadings

The primary objective of this exercise is to map pollutant loadings from ASMGHG into NWPCAM to estimate water quality effects at the national and regional levels. The initial assessment considered changes in N, P and TSS as representative of the most prominent nutrients and conventional pollutants. We focus entirely on cropland because ASMGHG reports county-level results for cropland only. Livestock manure loadings and afforestation are reported for the 63 ASMGHG regions, but we did not have the appropriate data at this time to enable a spatial disaggregation of manure loadings from the larger regions to the finer scale resolution of NWPCAM. We hope to be able to address this in future work.

3.2.1 GHG effects

Table 2 identifies the states associated with each region evaluated here. Table 3 presents GHG mitigation on cropland by each region under baseline and the two incentive prices (\$2.72 and \$15). GHGs are summed across the three component species (CO₂, CH₄, and N₂O) in Table 3. As indicated in Table 1, CO₂ is the dominant factor in agriculture and forest GHGs. Positive values of GHG indicate net emissions, negative values indicate net sequestration. The West North Central region has the largest baseline GHG emissions. All regions show some GHG mitigation response, but the largest effects are found in the West North Central, East North Central, and West South Central regions.

3.2.2 Pollutant Loadings

Table 4 presents N,P, and TSS cropland loadings by region. By and large there are two discernible patterns. First, there is considerable regional heterogeneity in the pollutant loadings associated with GHG mitigation. Some regions show substantial declines in loadings across all pollutants in response to the GHG incentive (e.g., East North Central), while others show an increase in loadings at both prices (e.g., Phosphorous in the East South Central region). Second, the regional heterogeneity differs somewhat across the two price scenarios. For example, the North West Central region exhibits an increase in loadings of all pollutants at the low incentive price, but then produces a significant reduction at the higher price. The pattern is reversed in the South Atlantic region, where there is a modest decline in all loadings at the low price, but an increase in loadings at the high price.

These heterogeneous results reflect two complicating factors

1. Variations in regional comparative advantage in agricultural production and GHG mitigation cause inter-regional shifts in production activities in response to the GHG incentives.

2. Some activities that enhance GHG benefits have some offsetting water quality costs where for example runoff may increase or greater infiltration of water to soils caused by increased organic matter and water holding capacity might over time increase nitrate infiltration into ground water.

The first factor reflects the spatial and cross-sectoral equilibrium aspects of ASMGHG. The model allows prices of agricultural commodities to increase as agricultural supply falls because of the change in management practices and land use change. In some circumstance (e.g., the Southeast under the higher price scenario), the indirect response caused by these agricultural price effects may more than offset management responses due to GHG incentives, thereby leading to a net increase in the loadings of some pollutants.

4. NWPCAM Results

Over the last decade, RTI has developed NWPCAM to provide EPA with an operational tool designed to provide watershed-based assessments of federal regulatory policies for water pollution control at the regional and national scales. NWPCAM provides a consistent national-scale water quality model framework for simulating the effects of point and nonpoint source pollutant loads on water quality in the streams, rivers, lakes, reservoirs, and estuaries of the United States. The model framework, based on the powerful EPA Reach File (RF1, RF3) databases of surface waters, is designed to provide information on changes in water quality conditions and the associated economic benefits resulting from implementation of the regulatory policies of the Clean Water Act.

Following the basic “blueprint” developed during the 1990s that outlined the components of a national-scale water quality model for pollutant transport and fate, the model framework for NWPCAM has been under development for several years. The model framework has evolved, and will continue to evolve, to incorporate lessons learned from earlier versions; new data, information and knowledge as it becomes available (in particular the National Hydrography Dataset which will supercede the Reach File system); improved model components; and changes in regulatory and policy requirements.

The basic approach for incorporating ASM results into NWPCAM is to use the ASM outputs to develop percent changes in the pollutants, and then apply these percentage changes by county to agricultural land cover cells in NWPCAM. Three sets of land cover files are used

1. The baseline loadings, which is unchanged;
2. Agricultural export coefficients adjusted for carbon pricing scenario 1; and,
3. Agricultural export coefficients adjusted for carbon pricing scenario 2.

The land use cells with the corresponding export coefficients are linked to the RF3 reach network, and are then routed down to the Reach File Version 1 (RF1) subset network. NWPCAM Version 1.1, which uses operates RF1, has been upgraded to model TN and TP; it already models TSS. NWPCAM 1.1 is then run on the three conditions of baseline, scenario 1 and scenario 2. Various maps and analyses of in-stream changes in water quality are then performed.

This process of incorporating ASM into NWPCAM accomplishes several things. The changes in loadings will occur in NWPCAM in a spatial pattern that reflects land use within the given county. For instance, if most of the agricultural land is in the southeast portion of the county, then that is where most of the loadings changes will take place. These loadings changes will then be associated with river reaches that correspond to the areas where the predominant agricultural land use is. That is, using the example, the reaches in the southeast portion of the county will experience the greatest changes due to ASM. For example, the northern portion of the county may be in one watershed and the southern portion in another watershed, and the loadings changes will thus properly wind up in the southern watershed.

Three NWPCAM NPS loadings databases are constructed for the instream water quality analyses. The first database contains “baseline” loadings, in which the default NWPCAM land cover cell export values are routed to the RF1 Database and then summed by RF1 Reach. The second and third sets multiply, by county, the agricultural land cover cells for each scenario’s

- TN, TP, and TSS concentration changes between baseline and scenario 1
- TN, TP, and TSS concentration changes between baseline and scenario 2

Metrics for water quality

Water quality effects can be evaluated in terms of changes in loadings, changes in concentrations, concentrations compared to criteria or thresholds, and water quality indices. In this round of analysis, change in in-stream nutrient concentrations are used to illustrate water quality effects.⁴ Annual loadings or the “flux” from ASMGHG is processed through NWPCAM at the mean annual flow rates, which reflect annualized changes, for every reach. Flux is essentially the in-stream concentration multiplied by the flow rate. It also possible to compute flux values (loadings per year) on a reach-by-reach basis because NWPCAM contains both estimates of mean annual flow for each reach and modeled nitrogen, phosphorous, and total suspended solids concentrations.

⁴EPA has not yet developed nutrient criteria by “nutrient ecoregions” for the entire country. Consequently RTI is using best professional judgement for the time being, and will compare NWPCAM in-stream concentration calculations to EPA’s nutrient concentration criteria, when available.

NWPCAM summaries can be performed at various scales, and grouped, for instance, by Hydrologic Region (there are 18 Hydrologic Regions in the continental United States). Summaries can include changes in loadings at the overall cell, RF3 Reach, RF1, and Hydrologic Region levels. In Appendix B, we report results at the national level.

Overview of Modeling Results

Appendix B presents 9 maps to illustrate baseline and changes in in-stream concentrations (for both GHG scenarios) for nitrogen (N), phosphorous (P), and total suspended solids (TSS). The baseline maps clearly follow a pattern of higher concentrations in farming regions as well as along the Southeast coastline; these are reasonable and follow what should be considered well-known patterns. The baseline maps indicate that the complex processes used to derive loadings and perform the instream modeling are in general working properly - a critical QC check. While it does not in itself provide a complete model validation, it does lead to a strong sense that model performance is reasonable, especially at a national scale.

The maps for changes in instream concentrations for the GHG incentives scenarios are very useful in that they show much more “texture” as to where water quality changes are occurring than can be shown by tables or graphs. As would be expected (and hoped), the instream concentration changes in scenario 2 are more significant than the changes in scenario 1. The changes in scenario 1 for P are primarily in the Upper Missouri Basin and in Wisconsin. TSS is similar but also shows changes in the southeastern U.S., Oklahoma, and eastern Kansas. N changes are fairly scattered in the 0-1 mg/l range.

Scenario 2 shows significant changes in P in the Upper Missouri basin, Upper Mississippi, Mid-Texas, and northern Nevada and California. Less significant but clear changes show up in the Ohio Valley and southeastern U.S. N is similar to P, with additional changes in Maine. TSS shows the same changes as above as well as Kansas, Iowa, the Lower Mississippi, and the Pacific Northwest.

There is a great deal of data behind this data, and future work will address a fuller interpretations of these results. Note, the maps illustrate one artifact of combining models that operate at different levels of spatial resolution. That is, in some cases (e.g. Illinois-Wisconsin) concentrations seem to change dramatically at state boundaries, presumably because ASM regions are defined by state boundaries whereas hydroregions cross state boundaries. While some attempts have been made to smooth these boundary effects, future work will investigate better methods to integrate the two models.

5. Summary

In this analysis, we have demonstrated that an agricultural and forest sector model can be combined with a water quality model to provide simultaneous estimates of GHG mitigation, sectoral response, regional production and associated water quality effects under GHG mitigation incentives in agriculture and afforestation. While the results here are quite preliminary, and cover a subset of land use activities and water pollutants, they do suggest that there are water quality “co-benefits” associated with GHG mitigation in the agricultural sector. However, at the prices evaluated here, the effects are somewhat modest and are unevenly distributed across the country. Both the GHG benefits and water quality co-benefits are highest in the North Central part of the U.S., where the agricultural has a large economic and environmental presence. Slight declines in water quality may be found in other regions, as economic forces re-allocate the more intensive production practices in response to inter-regional comparative advantage in crop production and GHG mitigation.

Several areas warrant further attention in future research, including

1. Inclusion of livestock manure loading and forest land loadings
2. Resolve scale and baseline differences between ASM and NWPCAM to ensure consistency of loading estimates from the regional level to the reach level
3. Evaluate alternative measures of water quality
4. Conduct more detailed analysis within the most heavily impacted regions (e.g., North Central)
5. Estimate monetized benefits of water quality improvements
6. Model T and P by incorporating other models, such as those of Walker (Walker, 1982, 1985, 1996)
7. Consider additional and enhanced outputs. For example, it would be instructive to develop specific maps in areas of particular interest, by various hydrologic and/or political breakouts. It is also possible to develop on-line computerized mapping outputs.

Appendix A: Overview of NWPCAM 1.1

Appendix A: Overview of NWPCAM 1.1

A modified version of NWPCAM 1.1 is used to model instream concentrations of TN, TP, and TSS in this project. NWPCAM 1.1 already contained the modeling of TSS, but did not model TN and TP. NWPCAM has been upgraded in this project to now also model TN and TP. This appendix summarizes NWPCAM in three sections. In section B-1, we present the model from the standpoint of the constituents modeled (TSS, TN, and TP) and the simplifying assumptions used in Version 1.1. In section B-2, we present the development of the non-point source data. In section B-3, we describe the process for estimating loadings of conventional pollutants.

A-1 Constituent Pollutants

NWPCAM 1.1 models several constituents that are not under consideration in this analysis, such as dissolved oxygen and fecal coliform bacteria. Only the constituents of concern in this project will be described below.

A-1.1 Total Suspended Solids (TSS)

Total suspended solids (TSS) are used as a surrogate indicator of water transparency to characterize recreational service flows provided by a water body. Low TSS concentrations are associated with a high degree of water clarity. High concentrations of TSS are generally associated with murky or turbid waters and are therefore important contributors to perceptions of poor water quality. The assessment of economic benefits is, in part, dependent on changes in water transparency (as assessed by TSS) and corresponding improvements that may result from implementing policy controls that reduce TSS loadings.

Simplifying Assumptions. In NWPCAM 1.1, no distinction was made as to the relative fractions of cohesive (clays and silts) and noncohesive (sands) particle sizes that contribute to deposition processes from the water column or the sediment bed concentration of solids that contributes to the resuspension of solids back into the water column. A simple net settling velocity was used to parameterize the interactions of particle size distributions with deposition and resuspension.

A-1.2 Total Nitrogen and Total Phosphorous

TN and TP are modeled using first-order decay kinetics, based on SPARROW (*SP*atially *R*eferenced *R*egression *O*n *W*atershed attributes) flow-dependent coefficients.

Simplifying Assumptions. The first-order decay model does not take algal uptake and loss into account, nor does it significantly model the differences between lakes and streams. The next generation of NWPCAM, 2.x, contains models that are much more robust, but correspondingly more complex. As a first-order approximation, the simplifying assumptions will still lead to much insight into the effects of the scenarios' effects on water quality.

A-2 Development of Nonpoint Source Data in NWPCAM

A-2.1 Data Sources

The basis for the land-use/land-cover spatial coverage used by NWPCAM 2.0 is the U.S. Geological Survey (USGS) conterminous United States Land Cover Characteristics (LCC) Data Set (Version 2). The LCC data set defines 26 land-use classifications as listed in Table 1-1. Land-use/land-cover data are defined at a square kilometer cell grid level in the LCC.

Each land-use cell is overlaid on Counties as well as assigned to the nearest routed RF3 reach for subsequent drainage area, stream discharge, and hydrologic routing purposes. As shown in the first column in Table 1-1, the 26 LCC land-use categories have been aggregated into eight categories in NWPCAM 2.0 to improve the tractability of the analysis. Land-use/land-cover data have also been used in NWPCAM for locating AFOs/CAFOs across the United States and for analyses of loadings from these point sources (see Section 5.0).

The USGS developed the LCC data set by classifying 1990 NOAA Advanced Very High Resolution Radiometer (AVHRR) satellite time-series images. Post-classification refinement was based on other data sets, including topography, climate, soils, and eco-regions (Eidenshink, 1992). The LCC data set is intended to offer flexibility in tailoring data to specific requirements for regional land-cover information.

Table 1-1. Modified Anderson Land Cover Classes and General Export Coefficients

Level 1 (derived)	Category (derived)	Level 2	Class	TN L	TN M	TN H	TP L	TP M	TP H
1	Agriculture	1	Dryland Cropland and Pasture	4	15	30	0.4	1.1	4
1	Agriculture	2	Irrigated Cropland and Pasture	4	15	30	0.4	1.1	4
1	Agriculture	3	Mixed Dryland/Irrigated Cropland and Pasture	4	15	30	0.4	1.1	4
2	Agriculture/ herbaceous	4	Grassland/Cropland Mosaic	3	12	25	0.4	1	3.5
3	Agriculture/ woodland	5	Woodland/Cropland Mosaic	3	10	20	0.2	0.75	2
4	Herbaceous	6	Grassland	3	5	10	0.3	0.6	3
4	Herbaceous	7	Desert Shrubland						
4	Herbaceous	8	Mixed Shrubland/Grassland	3	5	10	0.3	0.6	3
4	Herbaceous	9	Chaparral	3	5	10	0.3	0.6	3
4	Herbaceous	10	Savanna	3	5	10	0.3	0.6	3
5	Forest	11	Northern Deciduous Forest	1.75	2.5	3.75	0.1	0.2	0.3
5	Forest	12	Southeastern Deciduous Forest	1.75	2.5	3.75	0.1	0.2	0.3
5	Forest	13	Western Deciduous Forest	1.75	2.5	3.75	0.1	0.2	0.3
5	Forest	14	Northern Coniferous Forest	1.75	2.5	3.75	0.1	0.2	0.3
5	Forest	15	Southeastern Coniferous Forest	1.75	2.5	3.75	0.1	0.2	0.3
5	Forest	16	Western Coniferous Forest	1.75	2.5	3.75	0.1	0.2	0.3
5	Forest	17	Western Woodlands	1.75	2.5	3.75	0.1	0.2	0.3
5	Forest	18	Northern Mixed Forest	1.75	2.5	3.75	0.1	0.2	0.3
5	Forest	19	Southeastern Mixed Forest	1.75	2.5	3.75	0.1	0.2	0.3
5	Forest	20	Western Mixed Forest	1.75	2.5	3.75	0.1	0.2	0.3
6	Water Bodies	21	Water Bodies	4	10	30	0.2	0.3	1
4	Herbaceous	22	Herbaceous Coastal Wetlands	3	5	10	0.3	0.6	3
5	Forest	23	Forested Coastal Wetlands	1.75	2.5	3.75	0.1	0.2	0.3
6	Barren	24	Barren or Sparsely Vegetated	4	10	30	0.2	0.3	1
5	Forest	25	Subalpine Forest	1.75	2.5	3.75	0.1	0.2	0.3
7	Tundra	26	Alpine Tundra						
8	Urban (derived)	30	Urban	2	7.5	20	0.5	1.5	3.5

TN_L = total nitrogen export coefficient (low) TP_L = total phosphorus export coefficient (low)

TN_M = total nitrogen export coefficient (med) TP_M = total phosphorus export coefficient (med)

TN_H = total nitrogen export coefficient (high) TP_H = total phosphorus export coefficient (high)

A-2.2 Integrating Land-Use Cells and RF3

The image used to assign land-cover cells to an RF3 reach has a pixel size of 8-bit (1 byte), representing an area of 1 km². The image contains 2,889 lines and 4,587 samples covering the entire conterminous United States. Based on this information, it is possible to extract a specific area from the image into an ASCII file using an RTI-programmed C-computing language routine. This approach allows for importing only portions of the image, thereby reducing loading and processing time considerably compared to a full-image import with a commercial GIS package. The ASCII file then is used to generate a point coverage in ARC/INFO, which is converted to geographic coordinates to process it with existing RF3 reach coverages.

As noted, resolution of the land-use coverage data set is a square kilometer. The coverage for the continental United States comprises approximately 7,686,100 land-use cells at the square kilometer cell grid scale. The land-use coverage is overlaid on the RF3 hydrologic routing framework to associate each land-use cell with a specific RF3 reach (RF3Lite in the case of Hydroregions 8 and 17), watershed, and hydroregion. Each land-use cell is assigned to the nearest routed RF3 reach for subsequent drainage area, stream discharge, and hydrologic routing purposes. Information in the land-use/land-cover database includes the land-use/land-cover code for each cell, the watershed (HUC) code and county code (COFIPS) in which the cell is located, the RF3 reach (RF3Lite for Hydroregions 8 and 17) associated with the cell, and related information. On a hydroregion basis, each land-use/land-cover cell is given a unique identification number for modeling purposes. Table 1-2 lists the key fields and field descriptions for the land-use/land-cover database used by NWPCAM 2.0.

Figure 1-1 is a mosaic composite-overlay of RF3 reach, land-use/land-cover database, and county/watershed information represented at the spatial scale of an eight-digit HUC (watershed). Figure 1-1 depicts the general relationship of these data sets and information as integrated within NWPCAM 2.0. The foundation established by these relationships and the hydrologic routing function of the RF3/RF3Lite reach files enable the NWPCAM 2.0 user to conduct the various water quality modeling and economic benefits analyses developed within the modeling system. Current development activities involve porting the land-use/land-cover database used by NWPCAM 2.0 to an ORACLE relational database management system (RDBMS). Once completed, this change will improve the performance of NWPCAM 2.0 for analyses involving the land-use/land-cover database. A shortcoming of the current land-use/land-cover database is that the slope of a land-use cell is based on the average slope of first-order streams in the accounting unit in which the cell is located. Slope data are critical for computing overland travel times required for some water quality analyses. While using the average slope for the accounting unit is a reasonable approximation for these analyses, more representative and accurate analyses would be achieved if the slope for each land-use cell could

Land Use Cells and RF3 Hydrography in CU 07010201

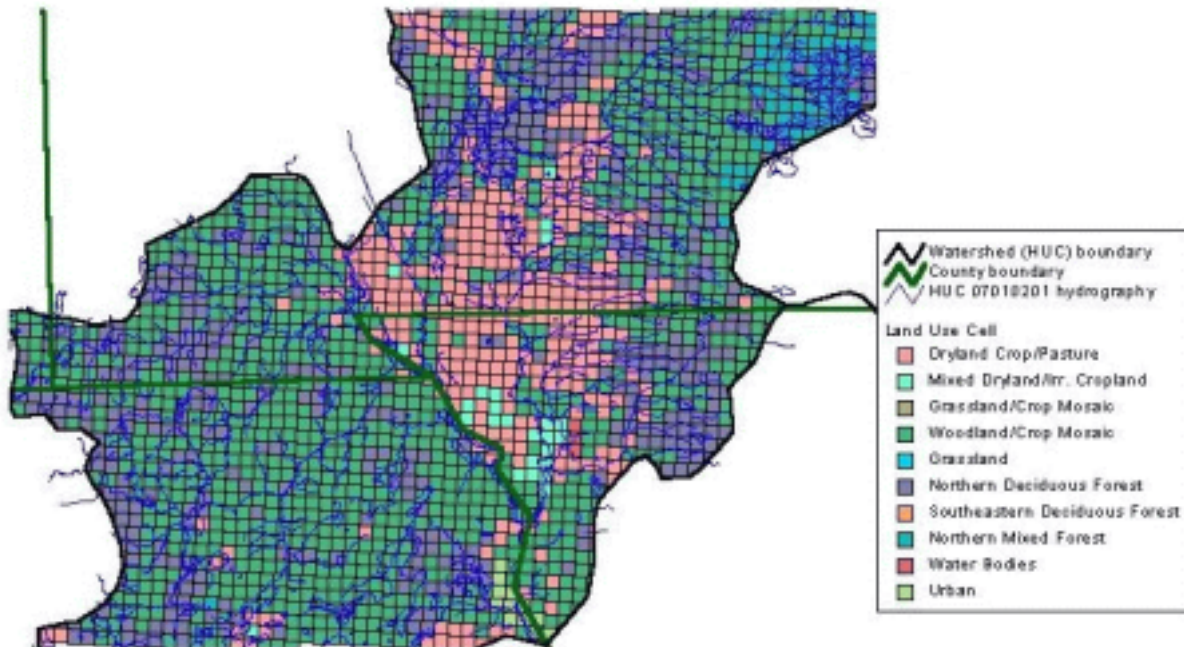


Figure 1-1. Mosaic Composite of Spatial Data at the Watershed (HUC) Level.

be computed. Possible future development activities could include establishing elevations for each land-use cell in the land-use/land-cover database for purposes of computing cell slopes.

A-2.3 Export Coefficient Models

The approach used in NWPCAM 2.0 for estimating nonpoint source loadings for both nutrients and conventional pollutants is based on an export coefficient model that is applied on a watershed level. Export coefficients are empirical, lumped-sum parameters that describe the loading of a given nutrient or pollutant in terms of mass per unit time per unit area. The specification of export coefficients requires estimates of both the unit loading and the area of land within a catchment described in terms of different types or classes of land use and/or land cover. The analytical model can be summarized as

$$L = \sum(EC_n \times A_n) \quad (4.1)$$

where

- L = loading to a reach (kg/yr),
 EC_n = export coefficient for category n (kg/ha/yr),
 A_n = area draining to reach in land use category n (ha), and
 n = land cover or use category.

A-3 Loadings Estimates for Conventional Pollutants

For conventional pollutants, export coefficients were assigned to three general land-use categories using values found in literature (see Table 1-3; Thomann and Mueller, 1987; Novotny and Olem, 1994). The three land-use categories were agricultural, forest, and urban areas. These values do not allow a breakdown of loadings into more detailed land use characterizations (e.g., grassland, pasture, feedlots, cropland). Therefore, the 26 LCC land-use categories were grouped into agriculture, forest, and urban categories (see Table 4-4). For mixed land-use categories (e.g., grassland/cropland mosaic, woodland/cropland mosaic), an average of the forest and agricultural runoff export coefficients was applied.

Table 1-3. Summary of Nonpoint Source Runoff Export Coefficients (kilogram/hectare/year)

Parameter	Urban	Agriculture	Forest
BOD5	34–90 (average 62)	26	5
TSS	360–672 (average 466)	1600	256

Nutrient loads for non-point sources were computed by land-use type by ecoregion based on SPARROW (*SP*atially *R*eferenced *R*egression *O*n *W*atershed attributes) which is a statistical modeling approach for estimating major nutrient source loadings at a reach scale based on spatially referenced watershed attribute data. An optimization algorithm was developed to estimate non-manure loadings by comparing SPARROW non-manure non-point source estimates for cataloging units with modeled outputs. The optimal coefficient set was determined for both nitrogen and phosphorus for each ecoregion within a hydroregion. This was accomplished by iteratively running an optimization routine using a genetic algorithm to estimate loading coefficients for major land use categories present in the ecoregion. Non-point sources were delivered directly to the RF3Lite reaches for hydrologic routing through the river/stream network. This process in effect calibrated the nutrient export coefficients in NWPCAM using the SPARROW model and produced the spatial variability represented in the data used to build SPARROW.

Non-point source data for fecal coliform, fecal streptococci, and sediments were not readily available at the national scale.

A-3.1 Revised Universal Soil Loss Equation (RUSLE)

The revised universal soil loss equation (RUSLE) was used to amend the export coefficients used for TSS loadings on agricultural land-use cells (USDA, 1997). This had the advantage of developing estimates of export coefficients that were spatially-variable. The RUSLE equation estimates average soil loss by the following equation:

$$\text{TSS} = R * K * L * S * C * P * 2241.7 \quad (1.1)$$

where

TSS = computed average soil loss (kg/ha/yr)

R = rainfall-runoff erosivity factor

K = soil erodibility factor

L = slope length factor

S = slope steepness factor

C = cover-management factor

P = support practice factor, including best management practices

The factors used in the RUSLE vary by climate, soil type, and other physiographic factors. Fifteen representative cities were selected to represent various climates across the US. The major land resource areas (MLRAs) were then overlaid with RF3 and related to a representative city using latitude/longitude coordinates. L and S are calculated values that vary with each stream reach (see Equations 1.2 to 1.3; USDA, 1997).

$$L = (\lambda/72.6)^m \quad (1.2)$$

where

λ = 1640 ft (the distance from centroid to edge of a land-use cell)

$m = \beta/(1+\beta)$

$\beta = (\sin\theta/0.0896) / (3\sin\theta^{0.8}+0.56)$

$\theta = \arctan(\text{slope})$

$$S = 10.8 \sin\theta + 0.03 \quad (1.3)$$

The values for R, K, and C were obtained from literature and vary by representative city (see Table 1-5; USACE, 1998). The P factor was assumed to be 1 for all cities.

A-3.2 Routing

Once the nonpoint source loadings were delivered to the corresponding RF3 reach, the loadings were routed through the RF3 reach network to the first downstream RF3Lite reach. These loadings to the RF3Lite reaches are then routed to the RF1 Network, which is a subset of RF3, and then transferred into the modified NWPCAM 1.1 that models with the RF1 network. Currently, nonpoint source loadings of conventional pollutants have been established for mean and summer flow conditions for all Hydroregions.

The TSS loadings were decayed via settling kinetics in routing from the RF3 network to the RF3Lite network.

$$C_t = C_0 H e^{(-K_{sed} * TOT)} \quad (1.4)$$

Table 1-5. Summary of RUSLE Factors by Representative City

Representative City	C	K	R
Amarillo	0.298	0.27	100
Atlanta	0.34	0.27	295
Bismarck	0.206	0.27	50
Boise	0.143	0.27	12
Charleston	0.359	0.27	400
Denver	0.214	0.27	40
Des Moines	0.309	0.27	160
Duluth	0.225	0.27	95
Fresno	0.113	0.27	12
Hartford	0.283	0.27	130
Helena	0.16	0.27	14
Las Vegas	0.035	0.27	8
Nashville	0.34	0.27	225
Portland	0.228	0.27	65
San Antonio	0.361	0.27	250

where

$$\begin{aligned}
 K_{sed} &= 0 && \text{velocity} > 0.3937 \text{ ft/sec} \\
 K_{sed} &= (0.3/\text{reach depth}) \times (1/0.304) && \text{velocity} < 0.0984 \text{ ft/sec} \\
 K_{sed} &= (0.3 / \text{reach depth}) \times (1 / 0.304) \times (0.0984 / \text{velocity}) && \text{velocity} > 0.0984 \text{ ft/sec} \\
 &&& \text{AND} < 0.3937 \text{ ft/sec}
 \end{aligned}$$

A-3.3 Summary

The incorporation of the RUSLE approach allowed spatial variation to be incorporated into loadings estimates for TSS. The result was a significant spatial distribution of TSS loadings on agricultural land. In the future, seasonal or monthly RUSLE formulation may be possible. Future work will attempt to incorporate spatial variability into estimates of BOD loadings as well.

Table 1-2. Key Fields of the Land-Use/Land-Cover Database

Field	Description
Cell_ID	Identification number assigned to land-use/land-cover cell for NWPCAM 2.0
REGnn_ID	Identification number to match cells in table with GIS coverage
LULC_CODE	Code describing type of land-use/land-cover for cell
AGCELL	Marker to designate agricultural land-use/land-cover cell
COFIPS	County FIPS code
DIST_FT	Distance from cell centroid to nearest RF3 reach (feet) (for overland flow calculations)
RF3RCHID	Identification number of nearest RF3 reach
CU	Catalog unit where cell is located
AU	Accounting unit where cell is located
SLOPE	Average slope of first order streams in accounting unit (for overland flow calculations)
RND_ID	Random number generated for agricultural cells in CU (for AFO/CAFO analyses)

Table 1. National summary of welfare, agricultural, and environmental impacts under three carbon dioxide price levels

	Unit	<i>Price per ton CO₂</i>		
		\$0	\$2.72	\$15
Agricultural Sector Welfare:				
US. Producer Welfare	billion \$	31.436	31.549	37.449
US Consumer Welfare	billion \$	1,179.947	1,179.103	1,173.896
Rest of the world Welfare	billion \$	256.836	256.620	255.453
Total Ag. Sector Welfare	billion \$	1,468.218	1,467.272	1,466.799
Agricultural Activities (using Fisher Index):				
Fisher Crop Production Index	Base = 100		99.22	95.27
Fisher All Goods Production Index (includes biofuels)	Base = 100		99.91	97.13
Fisher Crop Price Index	Base = 100		101.39	109.66
Fisher All Goods Price Index	Base = 100		100.68	106.53
U.S. Export Sales	billion \$	15.853	15.663	15.031
Land Use:				
DryLand	10 ⁶ acres	224.513	225.997	222.192
Irrigated Land	10 ⁶ acres	63.519	60.700	54.811
Pasture Land	10 ⁶ acres	386.990	390.172	390.929
Irrigation Water Use	10 ⁶ acres	79.419	76.823	67.106
Forest Land	10 ⁶ acres	0.000	0.026	14.220
Environment:				
Nitrogen	10 ⁶ tons	1,355.467	1,350.33	1,289.088
Potassium	10 ⁶ tons	6,568.171	6,711.274	6,467.575
Erosion	10 ⁶ tons	4,183.723	4,174.118	4,048.981
Phosphorus	10 ⁶ tons	4,693.678	4,682.225	4,480.945
Pesticide	10 ⁶ tons	8,905.296	8,846.094	8,562.836
Greenhouse Gas:				
CH4	MMTCE	44.627	44.213	41.916
CO2	MMTCE	38.208	-15.601	-131.459
N2O	MMTCE	45.628	42.626	40.707
Total	MMTCE	128.463	71.238	-48.836

Table 2. Regional Definitions

Census Region	States
East North Central	Illinois, Indiana, Michigan, Ohio, and Wisconsin
East South Central	Alabama, Kentucky, Mississippi, and Tennessee
Middle Atlantic	Connecticut, New Jersey, New York, and Pennsylvania
Mountain	Arizona, Colorado, Idaho, Montana, New Mexico, Nevada, Utah, and Wyoming
New England	Massachusetts, Maine, New Hampshire, Rhode Island, and Vermont
Pacific	Alaska, California, Hawaii, Oregon, and Washington
South Atlantic	Delaware, Florida, Georgia, Maryland, North Carolina, South Carolina, Virginia, and West Virginia
West North Central	Iowa, Kansas, Minnesota, Missouri, North Dakota, Nebraska, and South Dakota
West South Central	Arkansas, Louisiana, Oklahoma, and Texas

Table 3. GHG results from Cropland by Region

GHG totals (sum of CO₂, N₂O, and CH₄)
Quantities in million tons of carbon equivalent (MMTCE)
(Negative totals indicate a sink)

Census_Region	Levels		Change from baseline @		
	Baseline \$2.72	\$15.00	\$2.72	\$15.00	
East North Central	12.9	2.2	-2.0	-10.7	-14.9
East South Central	5.3	4.3	3.5	-0.9	-1.7
Middle Atlantic	2.4	1.4	1.2	-0.9	-1.2
Mountain	5.6	3.8	2.8	-1.8	-2.8
New England	0.1	0.1	0.0	-0.1	-0.2
Pacific	7.4	6.5	4.6	-0.9	-2.7
South Atlantic	4.2	2.5	1.4	-1.7	-2.8
West North Central	19.4	-5.8	-17.2	-25.2	-36.6
West South Central	12.2	8.7	3.2	-3.5	-9.0
Total	69.6	23.9	-2.3	-45.7	-71.9

Table 4. N, P and TSS loadings (million tons) from Cropland by Region**Nitrogen**

	Baseline	\$2.72	\$15.00	\$2.72	\$15.00
Census_Region					
East North Central	166.8	158.2	148.6	-8.6	-9.6
East South Central	185.2	184.2	188.9	-1.0	4.7
Middle Atlantic	109.3	111.4	109.2	2.0	-2.2
Mountain	99.5	97.3	91.2	-2.2	-6.1
New England	15.1	15.1	15.0	0.0	-0.1
Pacific	62.0	61.7	61.1	-0.3	-0.6
South Atlantic	165.6	163.0	166.0	-2.6	3.0
West North Central	213.9	222.8	208.2	8.9	-14.6
West South Central	335.2	333.9	298.2	-1.3	-35.7
Total	1,352.6	1,347.6	1,286.4	-5.0	-61.2

Phosphorous

	Baseline	\$2.72	\$15.00	\$2.72	\$15.00
Census_Region					
East North Central	983.7	954.3	921.9	-29.4	-32.4
East South Central	344.7	353.9	362.2	9.2	8.3
Middle Atlantic	207.4	210.9	212.6	3.5	1.7
Mountain	371.5	360.6	333.0	-10.9	-27.6
New England	23.2	23.2	24.0	0.0	0.7
Pacific	257.7	255.5	243.8	-2.2	-11.6
South Atlantic	329.5	326.0	331.5	-3.5	5.5
West North Central	1,380.3	1,404.3	1,349.6	24.0	-54.7
West South Central	787.8	785.7	694.7	-2.1	-91.0
Total	4,685.8	4,674.4	4,473.3	-11.4	-201.1

Total Suspended Solids

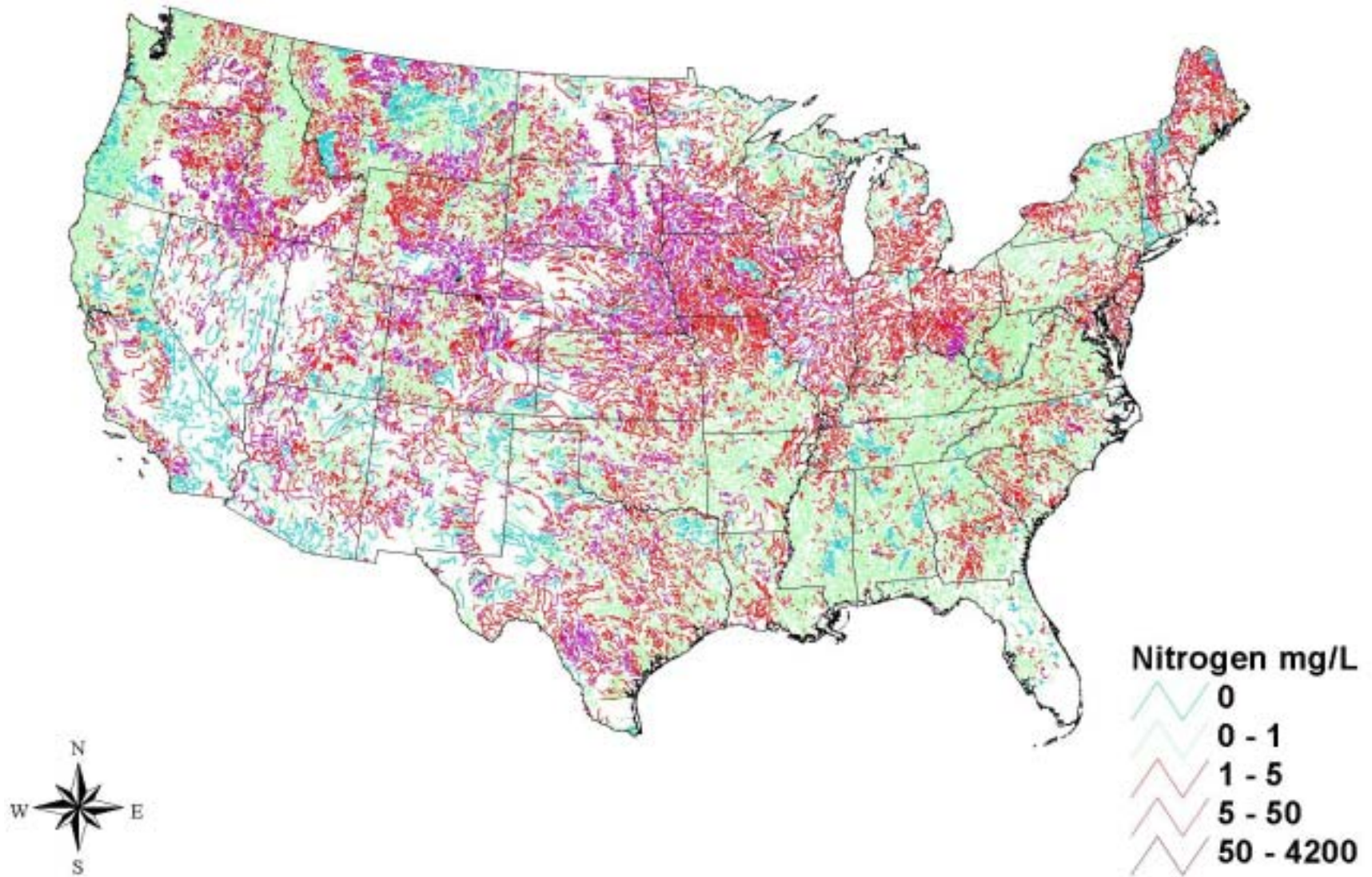
	Baseline	\$2.72	\$15.00	\$2.72	\$15.00
Census_Region					
East North Central	1,052.3	1,027.9	989.1	-24.4	-38.7
East South Central	247.7	246.4	249.8	-1.3	3.5
Middle Atlantic	92.8	91.3	96.0	-1.5	4.7
Mountain	27.8	27.3	26.8	-0.5	-0.5
New England	6.9	6.9	7.4	0.0	0.5
Pacific	89.5	92.8	98.3	3.3	5.5
South Atlantic	255.0	253.2	256.4	-1.8	3.2
West North Central	1,826.2	1,845.1	1,782.3	18.9	-62.8
West South Central	581.2	578.7	538.5	-2.5	-40.2
Total	4,179.4	4,169.6	4,044.6	-9.8	-125.0

References

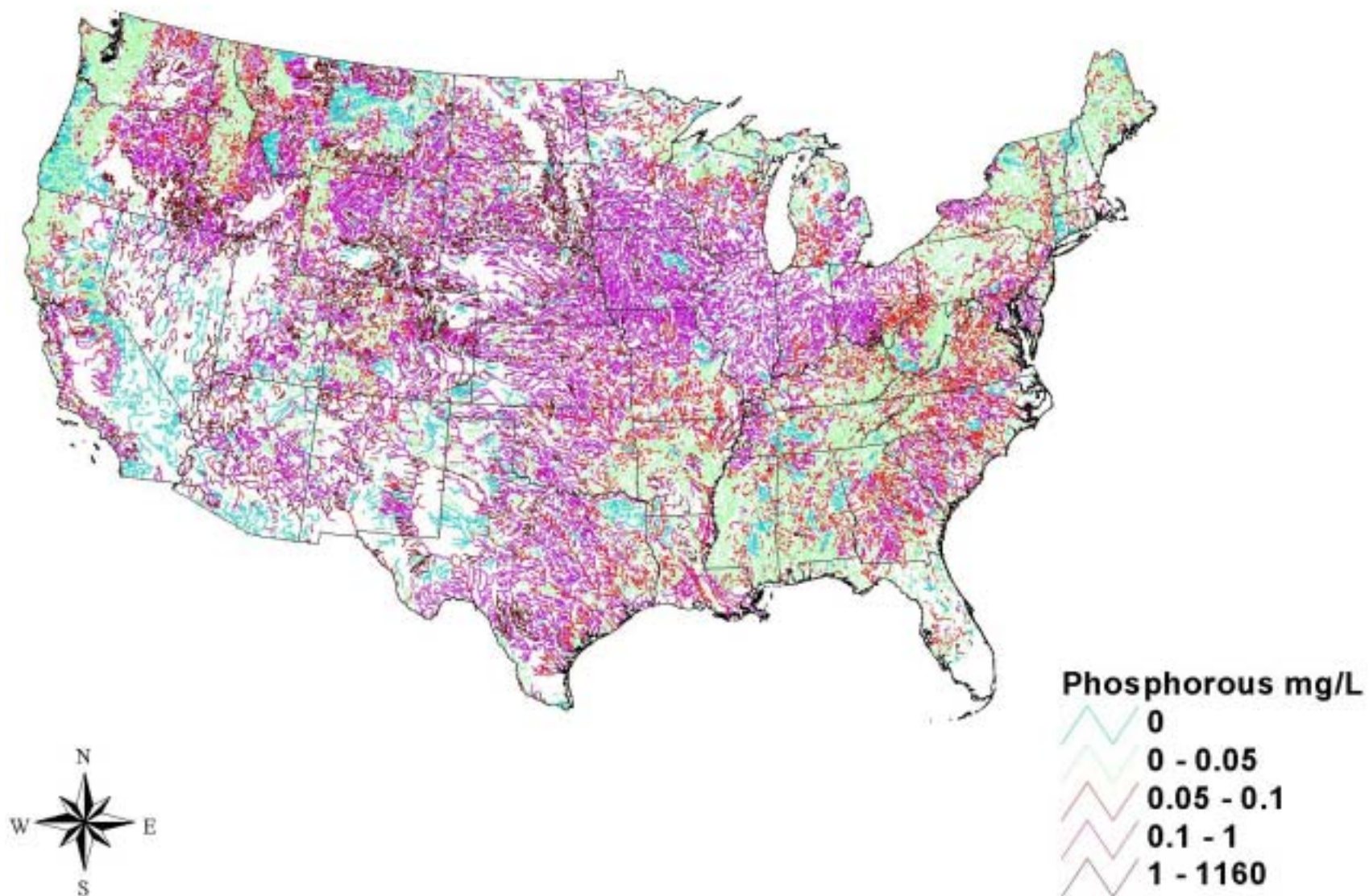
- RTI. 2000. National water pollution control assessment model (NWPCAM) Version 1.1. Final report prepared by Research Triangle Institute, Research Triangle Park, NC for U.S. Environmental Protection Agency, Office of Policy, Economics and Innovation, Washington, DC, November, RTI Project Number 92U-7640-031.
- U.S. Army Corps of Engineers (USACE). June 1998. "Analysis of Best Management Practices for Small Construction Sites." Work performed for the EPA Office of Wastewater Management.
- U.S. Department of Agriculture (USDA). 1997. *Predicting Soil Erosion by Water: A Guide to Conservation Planning With the Revised Universal Soil Loss Equation (RUSLE)*. Agriculture Handbook No. 703.
- Walker, W.W. 1982. "An Empirical Analysis of Phosphorus, Nitrogen, and Turbidity Effects on Reservoir Chlorophyll-a Levels." *Canadian Water Resources Journal* 7(1):88-107.
- Walker, W.W. 1985. *Empirical Methods for Predicting Eutrophication in Impoundments*. Report 3. Phase II: Model Refinements. U.S. Army Corps of Engineers Technical Report E-81-9. U.S. Army Engineer Waterways Experiment Station, Vicksburg, MS. Additional information available at <http://www.wes.army.mil/el/elmodels/emiinfo.html>.
- Walker, W.W. 1996. *Simplified Procedures for Eutrophication Assessment and Prediction: User Manual*. Instruction Report W-96-2, U.S. Army Engineer Waterways Experiment Station, Vicksburg, MS.

Appendix B: Maps of NWPCAM Modeling Results

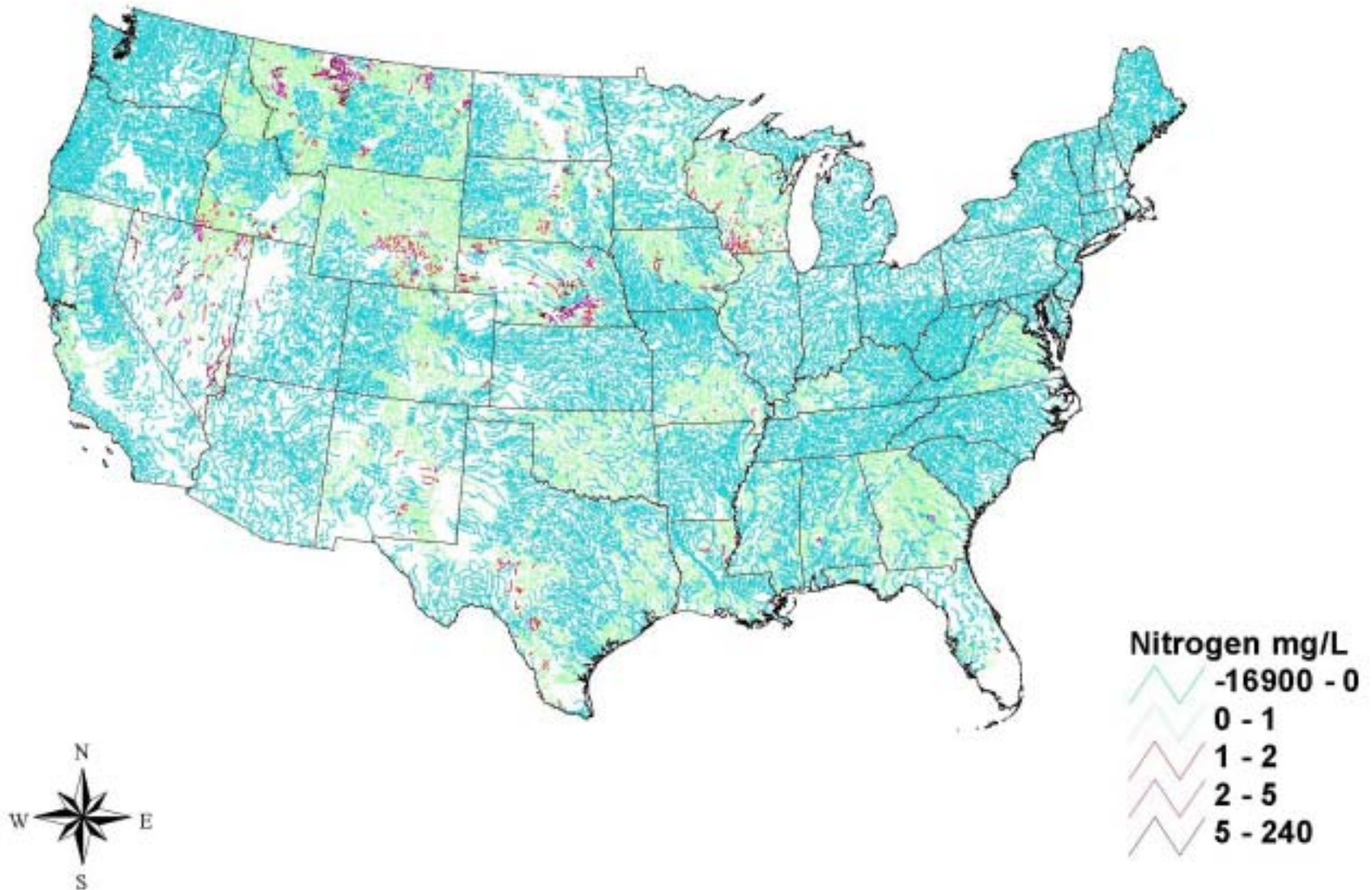
Baseline Nitrogen Concentrations



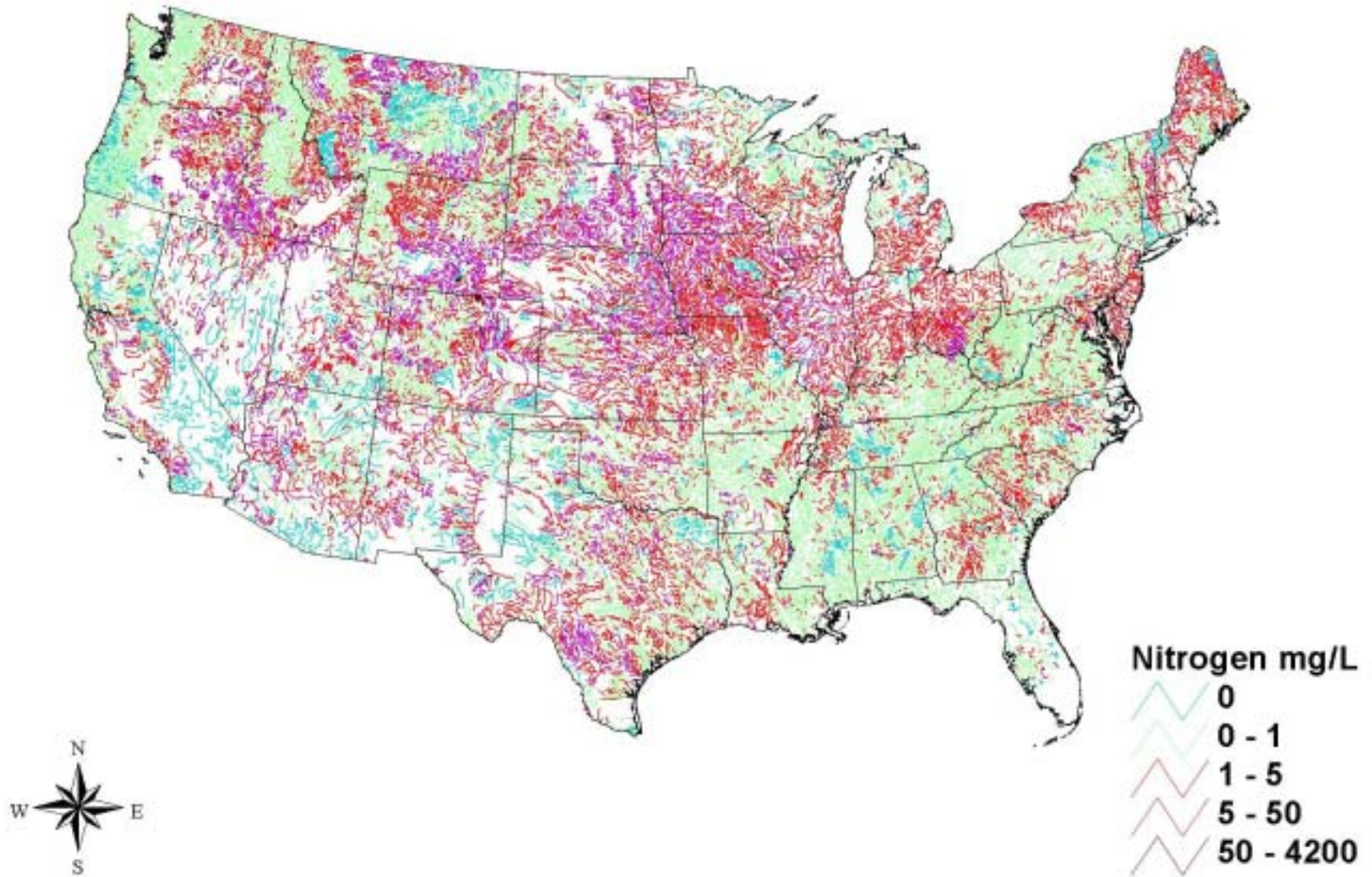
Baseline Phosphorous Concentration



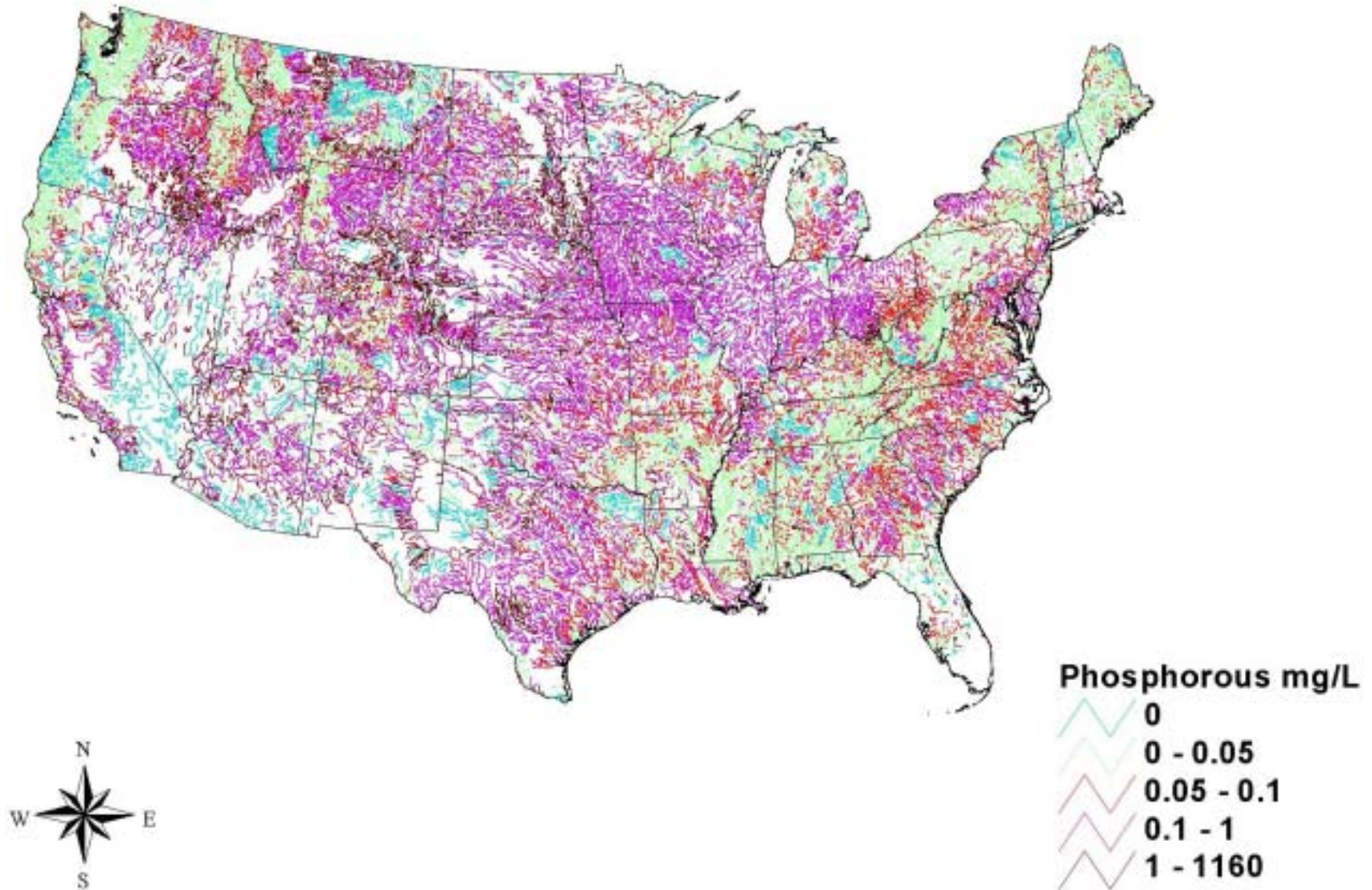
Change in Nitrogen Concentration Based on Scenario 1



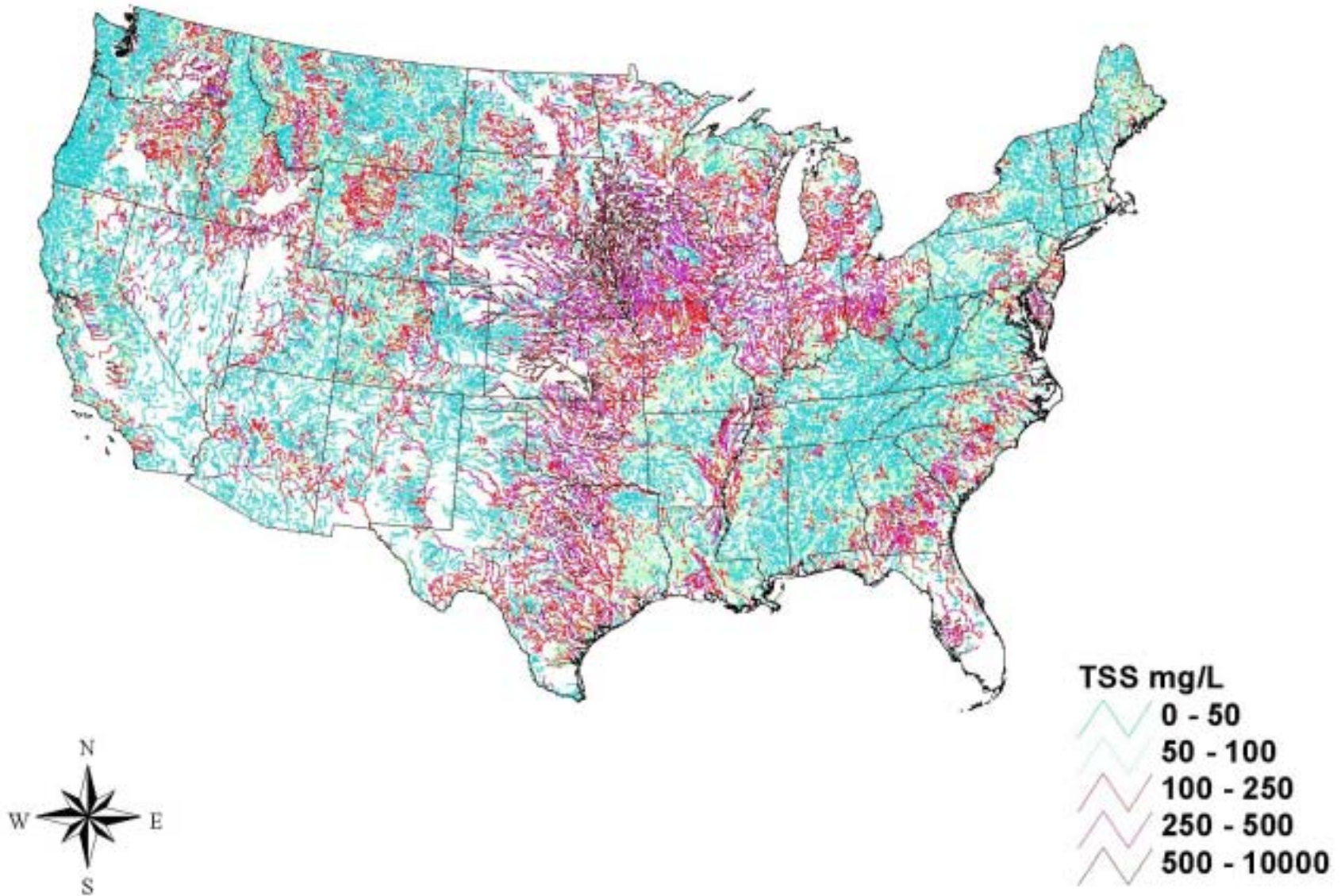
Baseline Nitrogen Concentrations



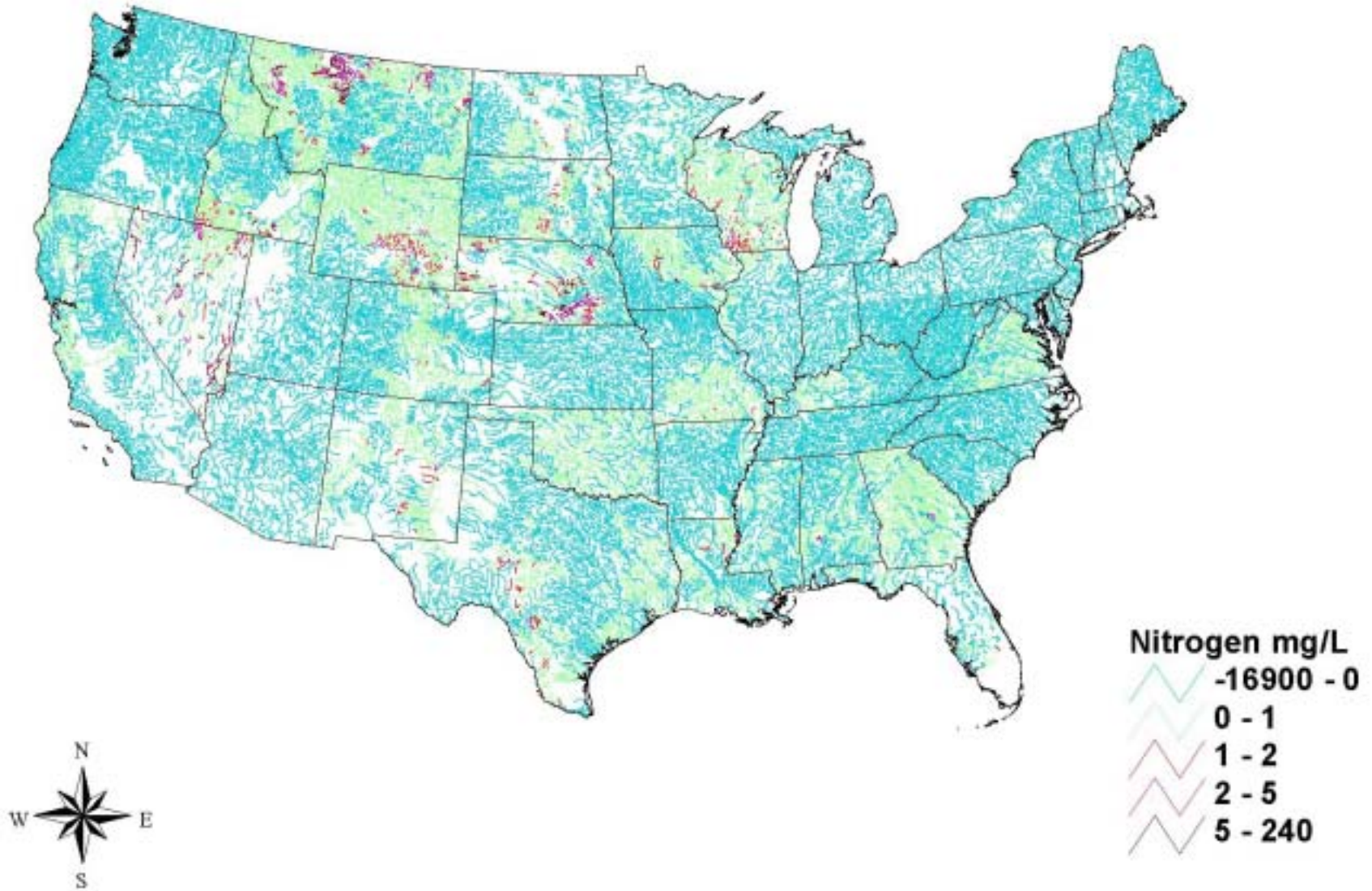
Baseline Phosphorous Concentration



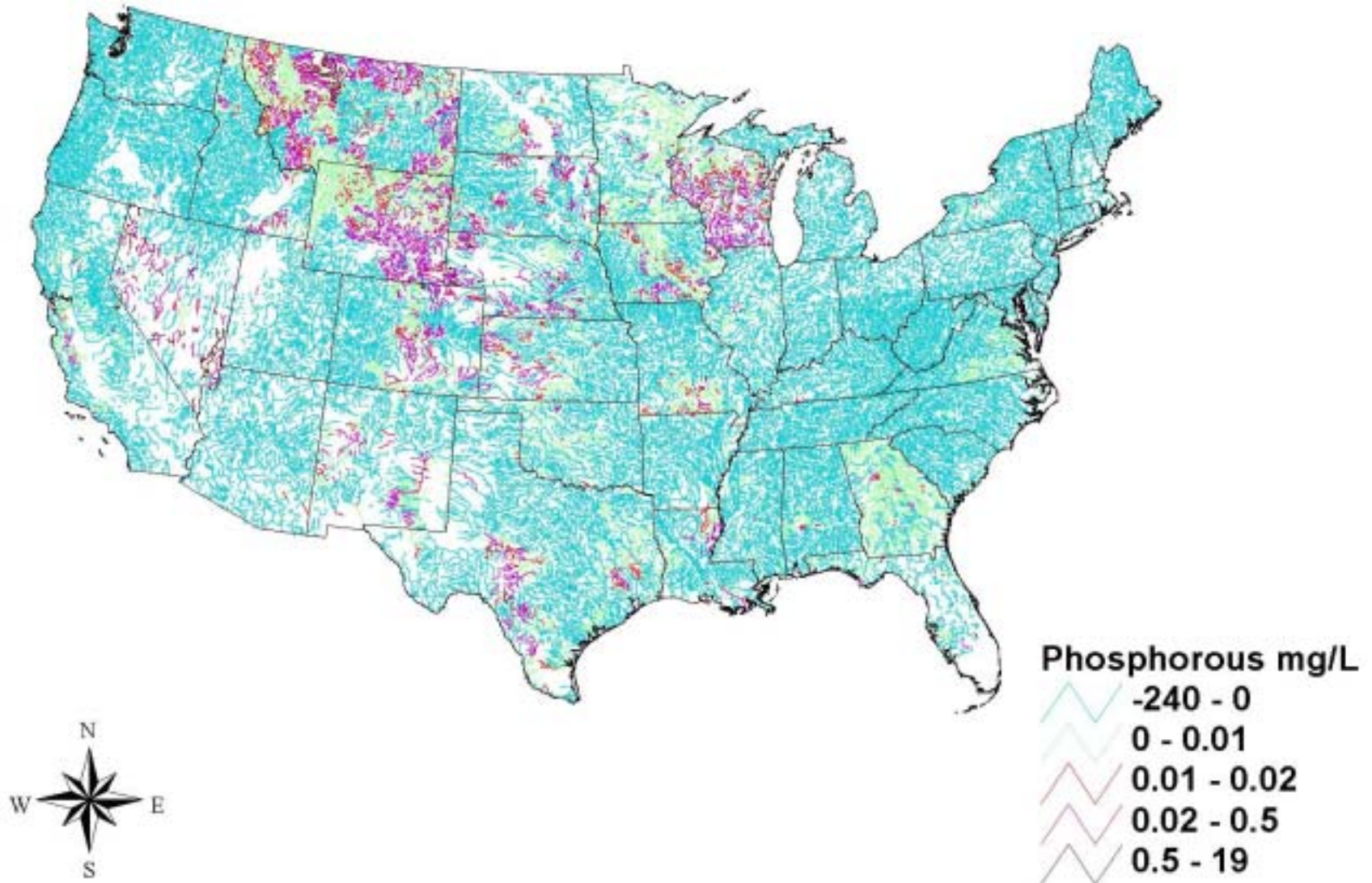
Baseline Total Suspended Solids (TSS) Concentration



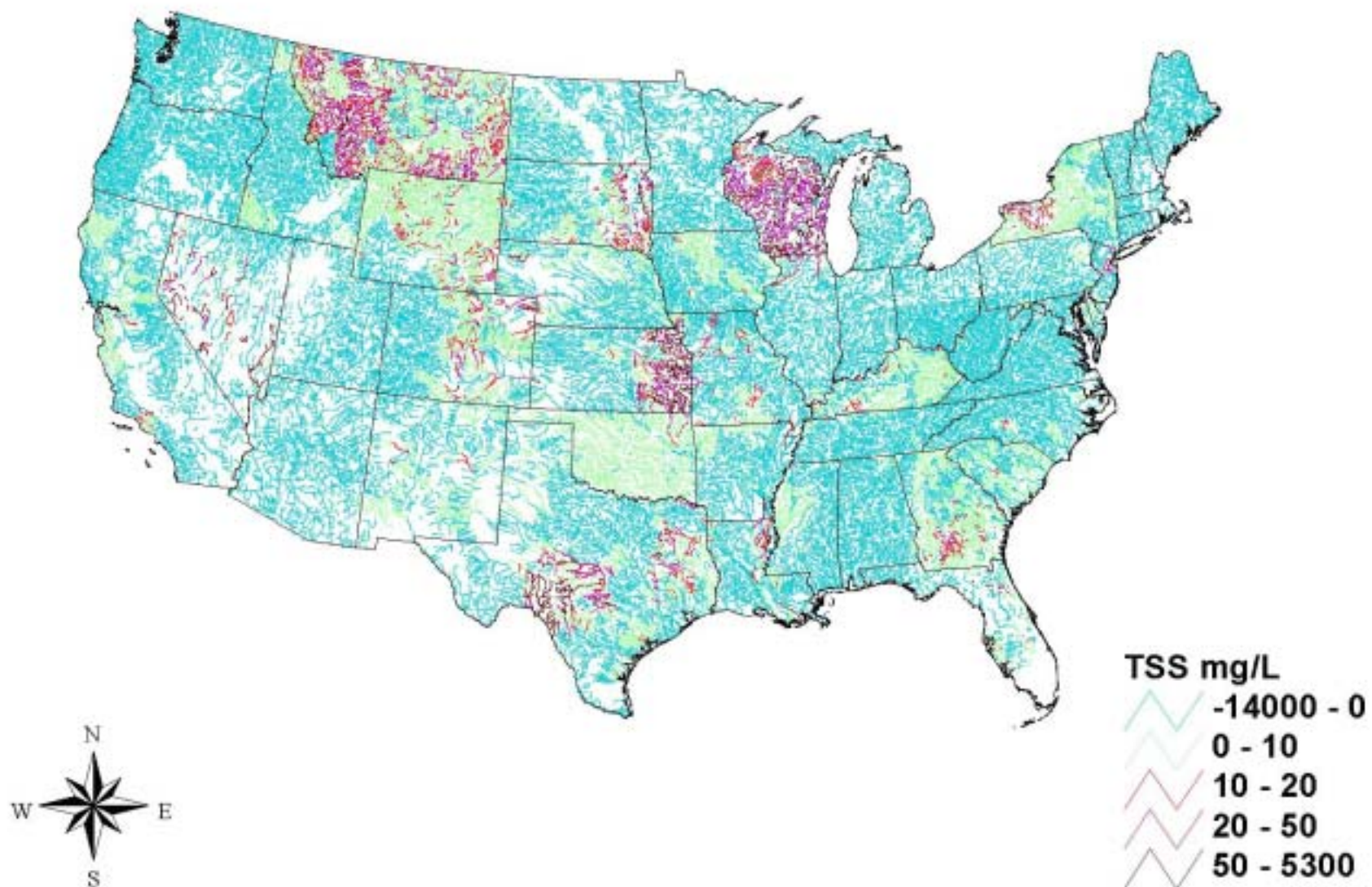
Change in Nitrogen Concentration Based on Scenario 1



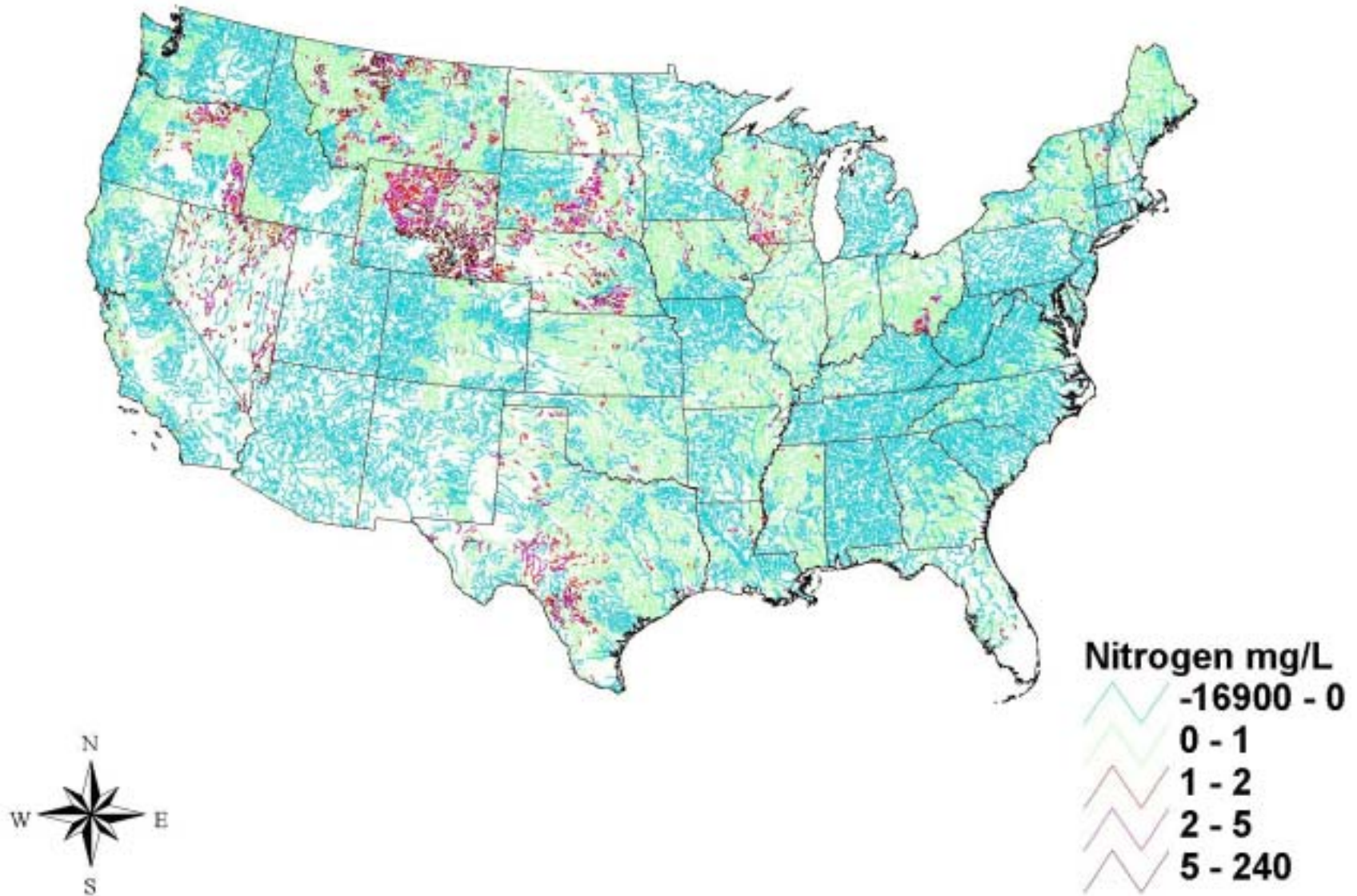
Change in Phosphorous Concentration Based on Scenario 1



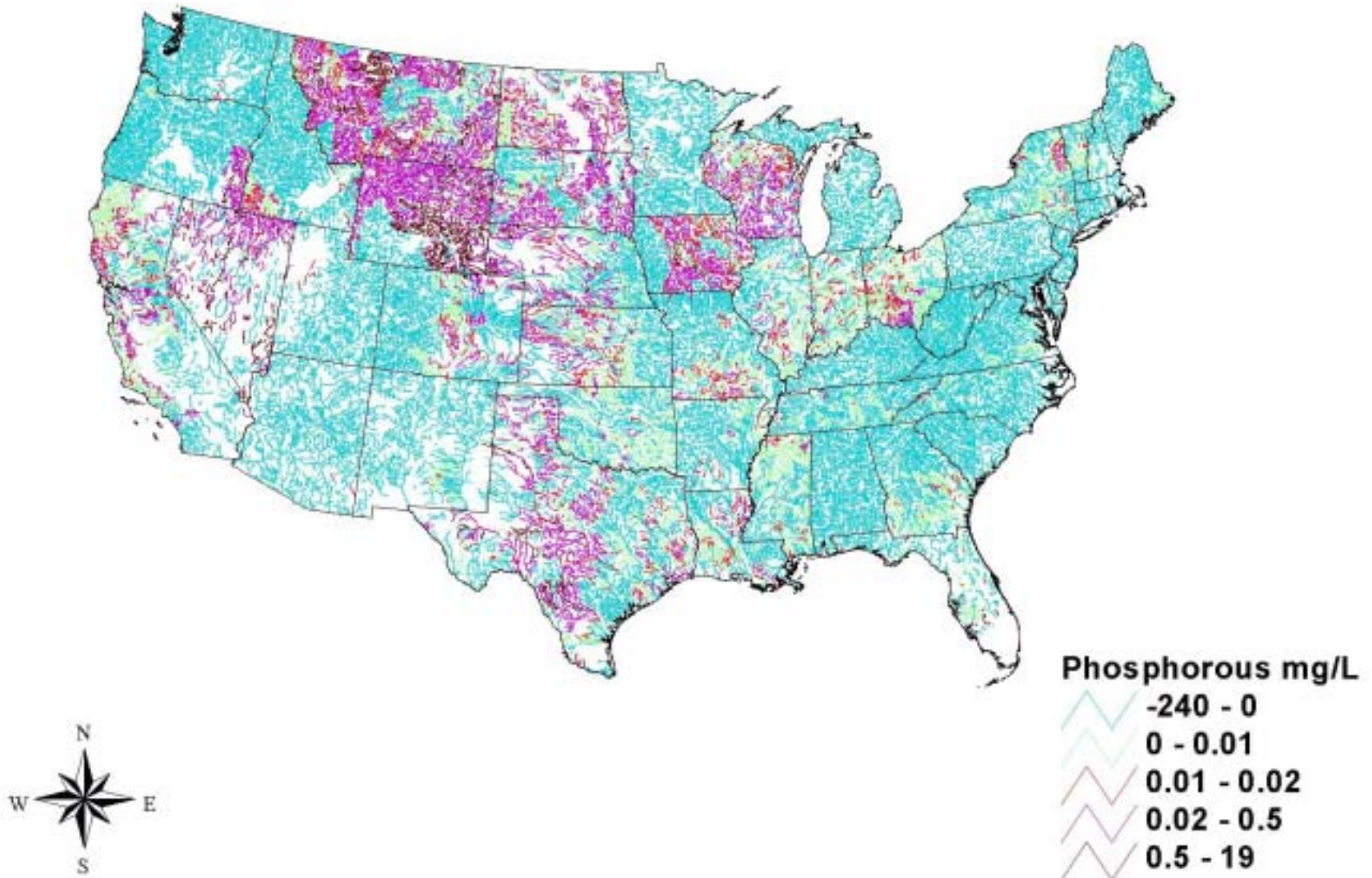
Change in Total Suspended Solids (TSS) Concentration Based on Scenario 1



Change in Nitrogen Concentration Based on Scenario 2



Change in Phosphorous Concentration Based on Scenario 2



Change in Total Suspended Solids (TSS) Concentration Based on Scenario 2

